Journal of Electroceramics, 6, 209–217, 2001

NO_x Sensing Properties of Varistor-Type Gas Sensors Consisting of Micro p-n Junctions

YASUHIRO SHIMIZU,* NOBUKUNI NAKASHIMA, TAKEO HYODO & MAKOTO EGASHIRA

Department of Materials Science and Engineering, Faculty of Engineering, Nagasaki University, 1-14 Bunkyo-machi, Nagasaki 852-8521, Japan

Submitted May 23, 2000; Revised February 27, 2001; Accepted March 7, 2001

Abstract. NO_x sensing properties of SnO_2-$x Cr_2O_3$ as a varistor-type gas sensor have been investigated in the temperature range of 200–600°C. The breakdown voltage of SnO_2 shifted to a higher electric field upon exposure to NO_2 at 300–500°C, and the largest breakdown voltage shift, i.e. the highest NO_2 sensitivity was observed at 400°C. In contrast, the direction of the breakdown voltage shift in NO varied with temperature: the breakdown voltage shifted to a lower electric field at 300°C, but to a higher electric field at 500°C, and remained almost unchanged at 400°C. The NO_2 sensitivity of SnO_2 was superior to the NO sensitivity at every temperature, and then the SnO_2 exhibited good selectivity to NO_2 at 400°C. The breakdown voltage of Cr_2O_3 shifted in the reverse direction upon exposure to NO and NO_2, in comparison with those observed with SnO_2, owing to its p-type semiconductivity. Thus, Cr_2O_3 also exhibited certain sensitivity to both NO and NO_2 at 200°C, being more sensitive to NO_2, though the sensitivities decreased drastically at temperatures higher than 300°C. The addition of 5.0 wt% Cr_2O_3 to SnO_2 resulted in a significant improvement of NO and NO_2 sensitivities at 600°C, being accompanied by an increase in the breakdown voltage in air. Especially, the NO sensitivity was superior to the NO_2 sensitivity in the concentration range of 20–100 ppm, and then SnO_2 mixed with 5.0 wt% Cr_2O_3 was found to be the most suitable candidate for a NO sensor among the sensors tested. The increase in the breakdown voltage in air induced by the Cr_2O_3 addition was confirmed to arise from both the decrease in the particle size of SnO_2 and the formation of micro p-n junctions at grain boundaries. The decrease in the particle size was also responsible for the increased NO and NO_2 sensitivities, but the p-n junctions were suggested to play a more important role in promoting and stabilizing the chemisorption of NO at higher temperatures.

Keywords: NO_x gas sensor, varistor, p-n junctions, nonlinearity, breakdown voltage

Introduction

Nitrogen oxides, NO_x (mainly NO and NO_2), are produced in combustion furnaces and automobile engines, and are typical air pollutants causing acid rain and photochemical smog. For effective control of both the combustion conditions and the NO_x-eliminating systems, there have been increasing demands for developing high performance, low-cost and solid-state NO_x sensors.

Several kinds of materials, e.g. semiconductor metal oxides and solid electrolytes, have so far been tested as a NO_x sensor. NO_2 always behaves as an oxidizing gas, and therefore its chemisorption leads to an increase in resistance of n-type semiconductive metal oxides used as a sensor material. On the other hand, NO chemisorbs as NO^-(ad) or NO^+(ad) depending on both the kind of semiconductive metal oxides and the temperature [1]. Under the conditions where NO and NO_2 show the opposite electronic nature upon adsorption, the sensitivity to a mixture of NO and NO_2, as in the case of the exhaust gases, becomes low or complicated, in comparison with the sensitivities to individual gases. In this case, the addition of catalysts to promote the oxidation of NO to NO_2 is a possible way to enhance the sensitivity to total NO_x. Even if both NO and NO_2 behave as an oxidizing gas under certain conditions, most of semiconductive metal oxides tend to exhibit

*To whom all correspondence should be addressed.

higher NO_2 sensitivity than NO [2–4]. The use of these semiconductor gas sensors is then limited in practical applications, because NO is the main component among NO_x species in the exhaust gases. Therefore, numerous efforts are now directed to developing gas sensors capable of detecting NO with high sensitivity and selectivity by employing semiconductor metal oxides [5] or stabilized zirconia equipped with oxide electrodes [6].

Our previous studies have been done to establish a new category of gas sensors, i.e. varistor-type gas sensors [7–14]. Conventional semiconductor gas sensors are usually operated at a very low electric field, e.g. less than several volts per mm of the thin-, thick- or bulk-type sensor materials, in detecting their resistance or conductance changes induced by the gases of interest. In the case of varistor-type sensors, however, the breakdown voltage in the nonlinear current-voltage characteristics of the sensor materials is measured under relatively high electric fields, and then the magnitude of the breakdown voltage shift induced by the gases of interest is regarded as a measure of the gas sensitivity. The breakdown voltage of porous ZnO-based varistors shifted to a lower electric field upon exposure to reducing gases, such as H_2 [9, 12], in the temperature range of 300–500°C, although no visible changes in the breakdown voltage were observed at temperatures lower than 200°C. In contrast, the breakdown voltage of the ZnO-based varistors shifted to a higher electric field upon exposure to oxidizing gases, such as O_3 and NO_2 [15–17], at elevated temperatures. Although NO sensing properties of several materials have also been studied as a varistor-type sensor [16, 17], all the materials tested, except for SnO_2 loaded with 5.0 wt% Cr_2O_3 [18], exhibited low NO sensitivity, in comparison with NO_2.

The present study is focused on the NO_x sensing properties of the SnO_2-Cr_2O_3 system. Microanalysis is also done to confirm the existence of Cr_2O_3 on the surfaces of SnO_2 grains and the formation of micro p-n junctions in the sensor.

Experimental

Preparation of Specimens

Tin dioxide powder was prepared from tin oxalate, obtained by the reaction between $SnCl_2 \cdot 2H_2O$ and $H_2C_2O_4$ in an aqueous solution, by pyrolysis at 400°C for 20 min in air and subsequent calcination at 1300°C for 2 h in air. Cr_2O_3 powder was prepared from $Cr(NO_3)_3 \cdot 2H_2O$ by pyrolysis on a hot plate at 300°C and subsequent calcination at 1300°C for 2 h in air. The resulting powders were milled in a planetary ball mill for 15 min by using yttria-toughened zirconia (YTZ) balls as grinding media.

Two methods were employed in preparing the mixed powder of SnO_2 and Cr_2O_3. In the case of the mixture of 1.0–10 wt% Cr_2O_3, a given amount of $Cr(NO_3)_3 \cdot 2H_2O$ was added to an aqueous suspension of the SnO_2 powder. The suspension was evaporated to dryness under stirring and then was subjected to pyrolysis at 300°C, followed by calcination at 800°C for 2 h in air. The resulting powder was milled in the planetary ball mill for 15 min. In preparing the mixture of 50 and 70 wt% Cr_2O_3, the powders of SnO_2 and Cr_2O_3 were mixed and milled in the planetary ball mill for 15 min, followed by calcination at 800°C for 2 h in air. Hereafter the binary specimens will be expressed as SnO_2-xCr_2O_3, where x represents the additive amount of Cr_2O_3 in wt%.

Fabrication of Varistor-Type Sensors

The powders thus prepared were mixed with a 5 wt% aqueous solution of polyvinyl alcohol at a level of 5 wt% and then pressed into discs of 5 mm in diameter and 0.8 mm thick. Thereafter the discs were sintered at 900°C for 1 h in air. The sintering condition adopted is rather mild compared with those for conventional dense ZnO-based varistors as the electric devices to limit transient voltage surges at room temperature. The mild sintering condition enables us to ensure the porous structure of the sintered discs, which is essential for their use as varistor-type gas sensors at elevated temperatures. Both faces of the sintered discs were polished down to 0.1–0.5 mm thick. Thereafter gold paste was applied to both faces (ca. 3 mm in diameter) and fired at 700°C for 30 min in air to serve as electrodes for electrical measurement.

Measurement of Current-Voltage Characteristics

Current (I)-voltage (V) characteristics of sensors were measured by scanning an applied dc voltage at a speed of 0.25 V s^{-1} in air and in 20, 40, 100 ppm NO or NO_2 balanced with air in the temperature range of 200–600°C. To prevent the sensors from suffering local

melting due to Joule heating, the measurement was stopped when the current flowing through the sensors reached 10 mA. The applied voltage was related to the electric field on the basis of the sensor thickness. For convenience, in this study the breakdown voltage is defined as the electric field at which the sensor conducts 10 mA. The gas sensitivity is then defined as the magnitude of the breakdown voltage shift induced by NO or NO_2 in air. The nonlinear coefficient, α, is calculated based on the following equation by using two applied voltage values at currents of 1.0 and 10 mA, respectively.

$$\alpha = 1/\log(V_{10\text{mA}}/V_{1.0\text{mA}}) \quad (1)$$

Characterization of Powders and Sintered Discs

Crystal phases of the powders used for fabricating sensors were characterized by X-ray powder diffraction (XRD) analysis (Rigaku, RINT-2000). The microstructure of the sensors was studied by scanning electron microscopic (SEM, Hitachi, S-2250N) observation of the fractured surfaces. In addition, transmission electron microscopy, equipped with an energy dispersive X-ray detector (TEM with EDX, JEOL, JEM-20210HT), was used to characterize fine structure at grain boundaries of SnO_2-5.0Cr_2O_3.

Results and Discussion

NO_x Sensing Properties

Figure 1 shows the *I-V* characteristics of SnO_2 in air as well as in various concentrations of NO and NO_2 at 300, 400, and 500°C. At 300°C, SnO_2 exhibited nonlinear *I-V* characteristics in every atmosphere, but the nonlinearity and the breakdown voltage in air tended to deteriorate with a rise in temperature. This behavior is quite reasonable, because the concentration of electrons available for conduction increases with a rise in temperature due to thermal excitation. The increase in the electron concentration in the bulk leads to a decrease in the depth of the space-charge region formed upon chemisorption of negatively charged species (O^-(ad) or O^{2-}(ad)) on the SnO_2 grain surface, and in turn a decrease in the height of double Schottky barriers at grain boundaries. Desorption of the negatively charged adsorbates with a rise in temperature may partially contribute to the decrease in the height of the double Schottky barriers. The breakdown voltage of SnO_2 shifted to a higher electric field upon exposure to NO_2, compared with that in air, at every temperature. This means the formation of negatively charged NO_2^-(ad), in addition to the oxygen adsorbates. The magnitude of the breakdown voltage shift, i.e. sensitivity, increased with increasing NO_2 concentration at every temperature. The highest sensitivity, ca. 165 V mm^{-1}, to 100 ppm NO_2 was observed at 400°C, as shown in Fig. 1(b). In contrast, the direction of the breakdown voltage shift induced by NO varied with temperature. The breakdown voltage shifted to a lower electric field at 300°C, but to a higher electric field at 500°C, suggesting the formation of NO^+(ad) and NO^-(ad) species on the surfaces of SnO_2 grains, respectively. At 400°C, the breakdown voltage remained almost unchanged upon exposure to NO. Thus, it was found that SnO_2 exhibited good selectivity to NO_2 at 400°C, but it was not useful as a NO sensor at every temperature.

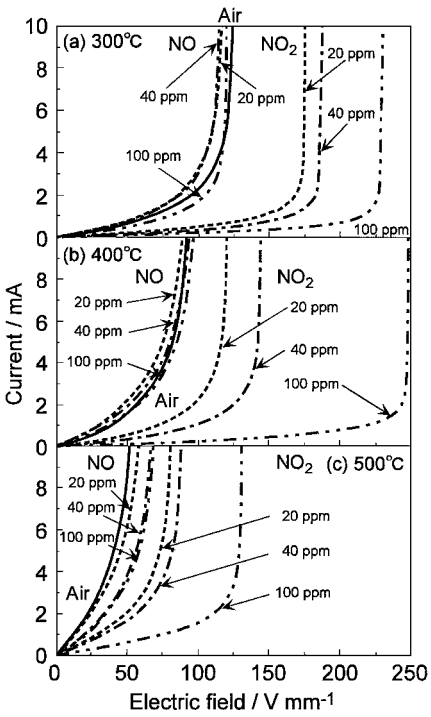

Fig. 1. I-V characteristics of SnO_2 in air and in various concentrations of NO and NO_2 at 300–500°C.

The *I-V* characteristics of Cr_2O_3 at 200–400°C are shown in Fig. 2. Cr_2O_3 exhibited good nonlinearity

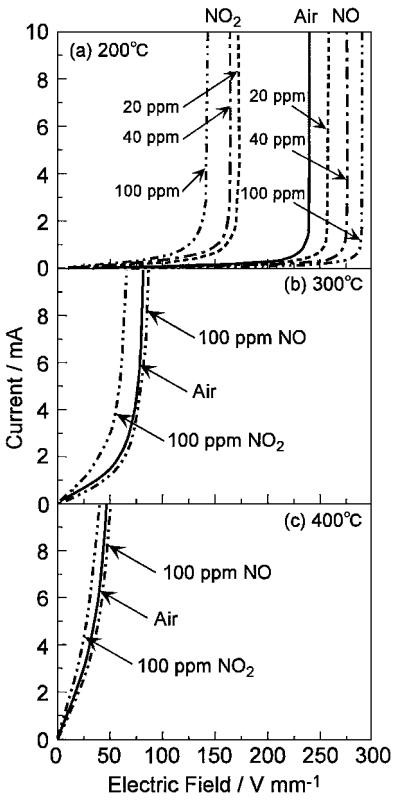

Fig. 2. I-V characteristics of Cr_2O_3 in air and in various concentrations of NO and NO_2 at 200–400°C.

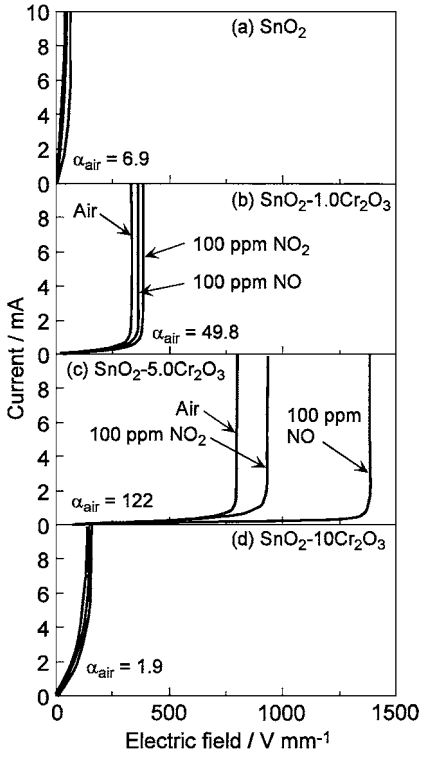

Fig. 3. I-V characteristics of SnO_2-xCr_2O_3 ($x = 0$–10.0) in air, 100 ppm NO and NO_2 at 600°C.

at 200°C in every atmosphere, but the breakdown voltage shifted in the reverse direction upon exposure to NO and NO_2, in comparison with those observed with SnO_2, owing to its p-type semiconductive nature. At 200°C, the NO sensitivity was relatively large, in comparison with SnO_2, but was still lower than the NO_2 sensitivity. The sensitivity of Cr_2O_3 to both NO and NO_2 decreased drastically with a rise in temperature above 300°C. It is considered that the difference in the temperature dependent sensitivity between SnO_2 and Cr_2O_3 reflects the different desorption behavior of NO and NO_2 from the surfaces of SnO_2 and Cr_2O_3 grains as well as the different temperature-dependence of the potential barrier height at the SnO_2-SnO_2 and Cr_2O_3-Cr_2O_3 grain boundaries in air. It was also found that Cr_2O_3 was not suitable for selective detection of NO among NO_x species.

Figure 3 shows the *I-V* characteristics of SnO_2 mixed with 1.0, 5.0 or 10 wt% Cr_2O_3 measured in air, 100 ppm NO and NO_2 at 600°C. For reference, the results obtained with SnO_2 are also shown in Fig. 3(a). At a temperature as high as 600°C, almost linear *I-V* characteristics were observed with SnO_2 in every atmosphere, and then SnO_2 was less sensitive to both NO and NO_2. Similar *I-V* characteristics and almost no sensitivity were observed with Cr_2O_3 at 600°C, although the data are not cited in Fig. 3. The addition of 1.0 wt% Cr_2O_3 to SnO_2 led to an improvement of the nonlinearity and the NO and NO_2 sensing properties, as shown in Fig. 3(b). With the addition of 1.0 wt% Cr_2O_3, the breakdown voltage increased from ca. 34 to 332 V mm^{-1} and the nonlinear coefficient from ca. 6.9 to 50. In addition, the breakdown voltage shift upon exposure to NO and NO_2 was in the same direction, that is to a higher electric field. SnO_2-1.0Cr_2O_3 exhibited sensitivity to both NO and NO_2, being more sensitive to NO_2, but the sensitivities were still low. More pronounced improvement of the sensing properties was achieved by the addition of 5.0 wt% Cr_2O_3, being accompanied by an increase in both the breakdown voltage and the nonlinear coefficient in air, as shown in Fig. 3(c). However, further addition of Cr_2O_3 resulted in decreases in the

breakdown voltage, in the nonlinear coefficient, and in the sensitivity to both NO and NO_2, as shown in Fig. 3(d).

Based on the *I-V* characteristics of all the sensors measured under different conditions, the operating temperature dependence of the breakdown voltage in air and the sensitivity to 100 ppm NO and NO_2 are plotted in Fig. 4. The breakdown voltage of SnO_2 in air was low, compared with those of SnO_2-$x Cr_2O_3$, and decreased with a rise in temperature, as mentioned above. The breakdown voltage of Cr_2O_3 in air was almost comparable to that of SnO_2 and exhibited a similar temperature dependence. However, the breakdown voltage of SnO_2-$x Cr_2O_3$ ($x = 1.0$–10) was higher than those of SnO_2 and Cr_2O_3 at every temperature. When compared at 600°C, the breakdown voltage initially increased with increasing Cr_2O_3, reaching a maximum at 5.0 wt%, and then decreasing to the level of SnO_2. Similar behavior is expected at temperatures lower than 500°C, although the breakdown voltage of SnO_2-5.0Cr_2O_3 could not be measured at temperatures lower than 500°C due to the problem associated with the measuring system employed in the present study. The reason for the increased breakdown voltage with Cr_2O_3 cannot be explained by a simple mixing model of SnO_2 and Cr_2O_3 grains. Regarding the NO sensitivity, several features can be emphasized from the results in Fig. 4(b). The SnO_2 was almost insensitive to NO in the temperature range of 300–600°C. However, the NO sensitivity increased with the addition of 1.0–5.0 wt% Cr_2O_3 at temperatures higher than 500°C, and the highest NO sensitivity at 600°C was achieved with SnO_2-5.0Cr_2O_3. This implies that the chemisorption of NO is promoted and then stabilized at higher temperatures by the addition of a small amount of Cr_2O_3. Formation of NO^-(ad) is expected under these conditions, provided that the SnO_2 specimens with 1.0−5.0 wt% Cr_2O_3 are n-type semiconductive. The NO sensing properties of the specimens with more than 50 wt% Cr_2O_3 became very similar to those of Cr_2O_3: the lower the temperature, the higher the NO sensitivity. This implies that the surface of SnO_2-$x Cr_2O_3$ ($x = 50$ and 70) is determined by the nature of Cr_2O_3 itself, and the formation of NO^+(ad) is suggested under these conditions. Nearly similar features were observed for the variation in NO_2 sensitivity with Cr_2O_3 concentration and operating temperature. However, chemisorption of NO_2 was not so much promoted, as compared with that of NO, by the addition of a small amount of Cr_2O_3. As a result, SnO_2-5.0Cr_2O_3 exhibited higher

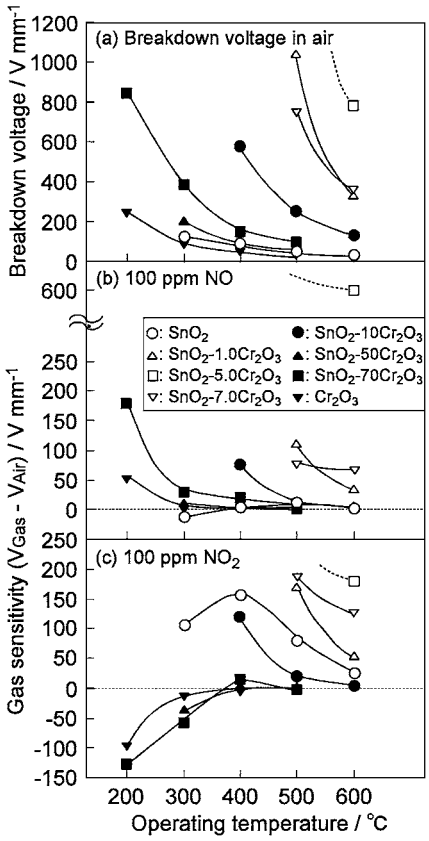

Fig. 4. Operating temperature dependence of (a) the breakdown voltage in air and the sensitivity to (b) 100 ppm NO and (c) 100 ppm NO of SnO_2-Cr_2O_3 disc specimens.

NO sensitivity than NO_2 at 600°C, as mentioned above.

Figure 5 shows variations in sensitivity of SnO_2-5.0Cr_2O_3 with NO and NO_2 concentration at 600°C. For comparative purposes, the results obtained with SnO_2 and SnO_2-1.0Cr_2O_3 are also shown. The NO sensitivity of SnO_2 was small and tended to saturate at 40 ppm. SnO_2-1.0Cr_2O_3 exhibited a slightly higher NO sensitivity than NO_2 at concentrations lower than 40 ppm, but the NO sensitivity also tended to saturate at higher concentrations, and the sensitivity to 100 ppm NO became lower than that to NO_2. In contrast, the NO sensitivity of SnO_2-5.0Cr_2O_3 was superior to the NO_2 sensitivity in the concentration range studied. In addition, an almost linear relationship between the NO sensitivity and the concentration could be obtained. Thus, it is confirmed that SnO_2-5.0Cr_2O_3 is the most suitable candidate as a NO sensor among the materials tested.

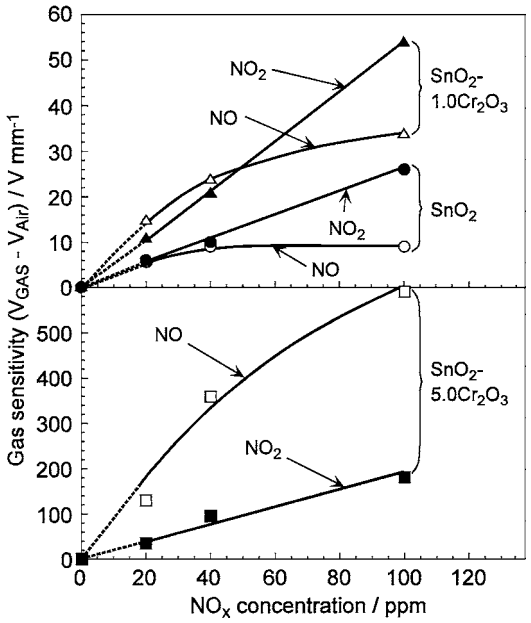

Fig. 5. Concentration dependence of NO and NO_2 sensitivities of SnO_2-$x Cr_2O_3$ (x = 0–0.5) at 600°C.

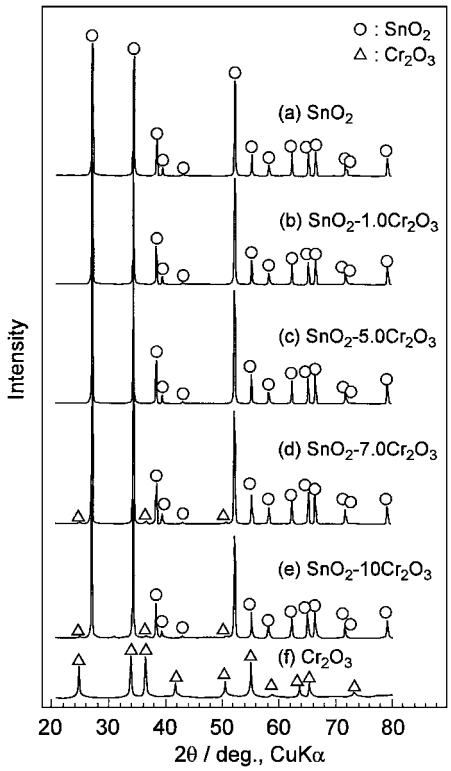

Fig. 6. X-ray diffraction patterns of SnO_2-$x Cr_2O_3$ powders.

Characterization

Phase and microstructural characterization of these sensors were conducted in order to obtain possible reasons for the change in the breakdown voltage in air induced by the addition of Cr_2O_3.

XRD patterns of the powders used are shown in Fig. 6. No phases other than SnO_2 were found in the powders containing less than 5.0 wt% Cr_2O_3, due to the detection limit of the spectrometer. Small Cr_2O_3 peaks were found in the powders containing more than 7.0 wt% Cr_2O_3, but formation of any mixed oxides was not found.

SEM photographs of the fracture surfaces of several sensors are shown in Fig. 7. The particle size of SnO_2 was not uniform and ranged from 0.28 to 2.9 μm with the average of ca. 1.1 μm, as shown in Fig. 7(a). Formation of small particles (ca. 0.2 μm) was found on the surfaces of SnO_2 grains by the addition of 1.0 wt% Cr_2O_3, as shown in Fig. 7(b). When 5.0 wt% Cr_2O_3 was added, the particle size of SnO_2 was reduced, and many small particles were observed on the surfaces of the SnO_2 grains. The decrease in the SnO_2 particle size means an increase in the number of SnO_2-SnO_2 grain boundaries in the sensor. The breakdown voltage in air is expected to increase with decreasing SnO_2 particle size, if the height of the potential barrier per grain boundary is assumed to be unchanged. Therefore, the decrease in the particle size can be considered a possible reason for the increase in the breakdown voltage induced by the addition of Cr_2O_3 up to 5.0 wt%. The number of small particles on the grain surface was further increased by the addition of 7.0 wt% Cr_2O_3, as shown in Fig. 7(d). Thus, most of these small particles are assumed to be Cr_2O_3 particles. Although it is not clear whether the particle size of SnO_2 is further reduced in SnO_2-7.0Cr_2O_3 and SnO_2-10Cr_2O_3, the surfaces of the SnO_2 grains are covered with small Cr_2O_3 particles. As mentioned before, the breakdown voltage of SnO_2-$x Cr_2O_3$ in air decreased with increasing Cr_2O_3 content after its maximum at 5.0 wt% Cr_2O_3. The formation of small Cr_2O_3 particles on the surfaces of SnO_2 grains may, therefore, be responsible for the decrease in the breakdown voltage in air of the SnO_2-$x Cr_2O_3$ ($x \geqq 7.0$).

Characterization of the fine structure at grain boundaries of SnO_2-5.0Cr_2O_3 was also conducted by employing TEM equipped with EDX. Figure 8 shows

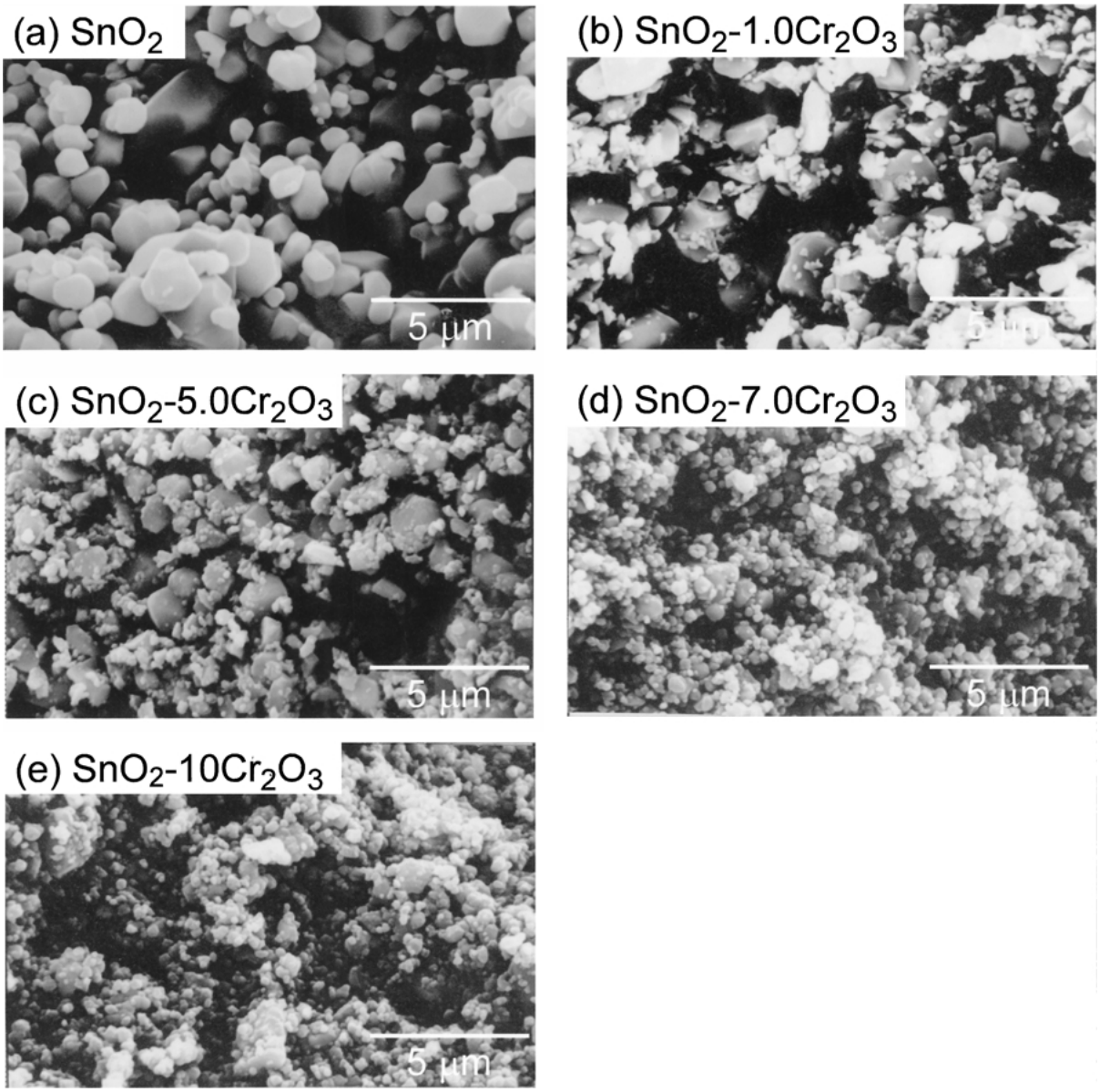

Fig. 7. SEM photographs of SnO_2-$x Cr_2O_3$ powders.

EDX patterns of the selected areas indicated by circles in the inserted TEM photographs. In these patterns Cu and Zr peaks come from a Cu grid and the YTZ balls used for milling the powder, respectively. From these data, relatively high Cr peaks were observed near grain boundaries, compared with those obtained on SnO_2 grain surfaces. Thus, Cr_2O_3 was found to segregate at grain boundaries. From these results, it is reasonable to consider that a number of micro p-n junctions are formed at the grain boundaries in SnO_2-5.0Cr_2O_3, given that Cr_2O_3 is p-type semiconductive. The formation of micro p-n junctions undoubtedly enhances the potential height at the grain boundaries, and therefore is anticipated to be responsible for the increase in the breakdown voltage in air.

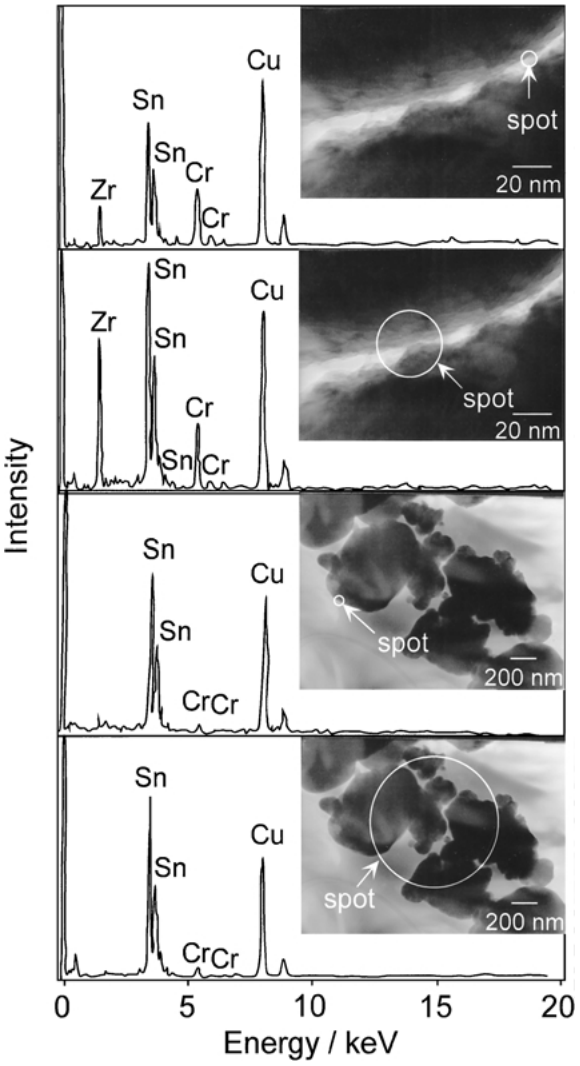

Fig. 8. EDX patterns at selected areas in SnO_2-5.0Cr_2O_3.

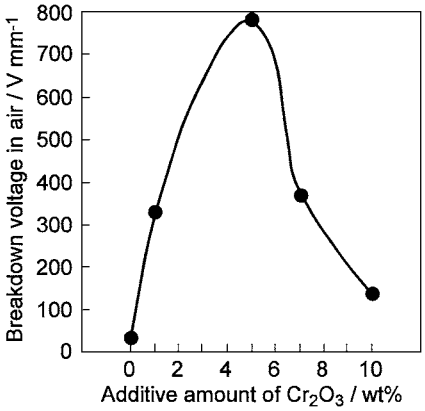

Fig. 9. Variation in the breakdown voltage of SnO_2-$x$$Cr_2O_3$ in air at 600°C with the additive amount of Cr_2O_3.

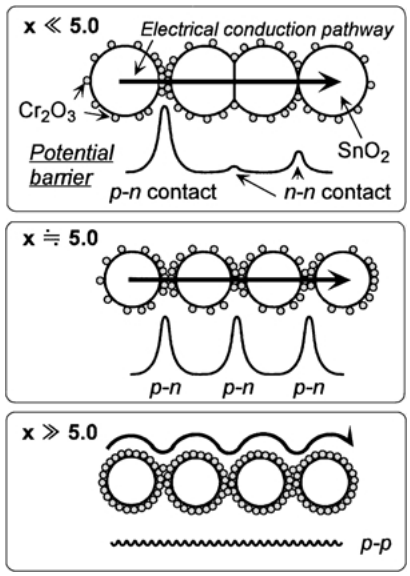

Fig. 10. Electronic conduction model of SnO_2-$x$$Cr_2O_3$.

Conduction Model

Figure 9 shows a variation in the breakdown voltage of SnO_2-$x$$Cr_2O_3$ ($x = 0$–10) in air at 600°C with the additive amount of Cr_2O_3. Based on the phase and microstructural characterization, the variation of the breakdown voltage can be explained by the conduction model schematically illustrated in Fig. 10. The increase in the breakdown voltage by up to 5.0 wt% Cr_2O_3 addition can be ascribed to both the decrease in the particle size of SnO_2, i.e. the increase in the number of SnO_2-SnO_2 grain boundaries, and the formation of micro p-n junctions, i.e. SnO_2-Cr_2O_3 contacts, at grain boundaries. It is anticipated that a number of micro p-n junctions are formed at grain boundaries of SnO_2-5.0Cr_2O_3, while surfaces of SnO_2 grains are not fully covered with small Cr_2O_3 particles. The maximum breakdown voltage of the SnO_2-5.0Cr_2O_3 may arise from these two factors. On the other hand, the decrease in the breakdown voltage above 7.0 wt% Cr_2O_3 may be due to the formation of a new, high conduction path consisting of p-p contacts, Cr_2O_3-Cr_2O_3 contacts, on the surfaces of SnO_2 grains. Although many p-n junctions should be formed at grain boundaries of the

SnO_2-$x Cr_2O_3$ ($x \geqq 7.0$), the formation of the high conduction path makes the effect of the p-n junctions less important.

The decrease in the particle size of SnO_2 induced by the addition of Cr_2O_3 undoubtedly leads to an increase in the adsorption sites for NO and NO_2 per unit volume of SnO_2 grains and in turn in the number of more sensitive grain boundaries. Thus, the increased NO and NO_2 sensitivity can be ascribed to the decrease in the particle size of SnO_2. However, the increment of the NO and NO_2 sensitivities induced by the addition of 5.0 wt% Cr_2O_3 was far larger than that expected from the decrease in particle size. Thus, it is anticipated that the micro p-n junctions offer new adsorption sites for NO and NO_2 besides those on the SnO_2 and Cr_2O_3 surfaces, although the mechanism is not clear at present. In addition, chemisorption of NO was more stabilized, in comparison with NO_2, at temperatures higher than 500°C apparently by the formation of the micro p-n junctions. The reason for this phenomenon is also not clear at present. Information on these two points would be very useful for designing more sensitive and selective NO varistor-type and/or semiconductor-type gas sensors. The surface chemistry of the micro p-n junctions is now under investigation.

Conclusion

A new varistor-type gas sensor capable of detecting NO with high sensitivity was developed by the addition of 5.0 wt% Cr_2O_3 to SnO_2. Both SnO_2 and Cr_2O_3 were more sensitive to NO_2 than to NO. The addition of 5.0 wt% Cr_2O_3 to SnO_2 resulted in a significant improvement of the NO sensitivity at 600°C, in comparison with the NO_2 sensitivity, being accompanied by an increase in the breakdown voltage in air. In addition, the NO sensitivity varied almost linearly with NO concentration up to 100 ppm. The decrease in the particle size of SnO_2 and the apparent formation of p-n junctions at grain boundaries were consistent with the microstructural characterization. The increase in the breakdown voltage in air induced by the Cr_2O_3 addition was attributed to arise from both the decrease in the particle size of SnO_2, i.e. the increase in the number of SnO_2-SnO_2 grain boundaries, and the formation of micro p-n junctions, i.e. SnO_2-Cr_2O_3 contacts, at grain boundaries. The decrease in the particle size was also held responsible for the increased NO and NO_2 sensitivities, but the p-n junctions were suggested to play a more important role in promoting and stabilizing the chemisorption of NO at higher temperatures.

Acknowledgment

The financial support from a Grant-in-Aid for Scientific Research (B) (No. 12450270) from Japan Society for the Promotion of Science is greatly appreciated.

References

1. M. Akiyama, J. Tamaki, N. Miura, and N. Yamazoe, *Denki Kagaku (presently Electrochemistry)*, **64**, 1285 (1996).
2. M. Akiyama, J. Tamaki, N. Miura, and N. Yamazoe, *Chem. Lett.*, **1991**, 1611 (1991).
3. C. Cantalini, M. Pelino, H.T. Sun, M. Faccio, S. Santucci, L. Lozzi, and M. Passacantando, *Sensors and Actuators B*, **35–36**, 112 (1996).
4. M. Penza, M.A. Tagliente, L. Mirenghi, C. Garardi, C. Martucci, and G. Cassano, *Sensors and Actuators B*, **50**, 9 (1998).
5. J. Tamaki, T. Nagaoka, Y. Yamamoto, and M. Matsuoka, *Trans. Inst. Elect. Eng. Jpn.*, **188-E**, 125 (1998) (in Japanese).
6. N. Miura, G. Lu, M. Ono, and M. Yamazoe, *Solid State Ionics*, **117**, 283 (1999).
7. F. Lin, Y. Takao, Y. Shimizu, and M. Egashira, *Denki Kagaku (presently Electrochemistry)*, **61**, 1021 (1993).
8. F. Lin, Y. Takao, Y. Shimizu, and M. Egashira, *Sensors and Actuators B*, **24/25**, 843 (1995).
9. F. Lin, Y. Takao, Y. Shimizu, and M. Egashira, *J. Am. Ceram. Soc.*, **78**, 2301 (1995).
10. M. Egashira, Y. Shimizu, Y. Takao, and Y. Fukuyama, *Sensors and Actuators B*, **33**, 89 (1996).
11. Y. Shimizu, E. Kanazawa, Y. Takao, and M. Egashira, *Trans. Inst. Elect. Eng. Jpn.*, **117-E**, 560 (1997).
12. Y. Shimizu, F. Lin, Y. Takao, and M. Egashira, *J. Am. Ceram. Soc.*, **81**, 1633 (1998).
13. Y. Shimizu, E. Kanazawa, Y. Takao, and M. Egashira, *Sensors and Actuators B*, **52**, 38 (1998).
14. T. Hyodo, E. Kanazawa, Y. Takao, Y. Shimizu, and M. Egashira, *Electrochemistry*, **68**, 24 (2000).
15. M. Egashira, Y. Shimizu, Y. Takao, and S. Sako, *Sensors and Actuators B*, **35/36**, 62 (1996).
16. Y. Shimizu, T. Iwanaga, Y. Takao, and M. Egashira, *Trans. Inst. Elect. Eng. Jpn.*, **118-E**, 130 (1998).
17. T. Hyodo, K. Okamoto, Y. Takao, Y. Shimizu, and M. Egashira, *Trans. Inst. Elect. Eng. Jpn.*, **119-E**, 103 (1999).
18. T. Hyodo, N. Nakashima, Y. Shimizu, and M. Egashira, *in Proc. of the 4th East Asian Conf. on Chemical Sensors*, Nov. 23–26, 1999, Hsinchu, Taiwan (1999), p. 113.